Journal of
Synchrotron Radiation

ISSN 0909-0495

Received 5 December 2012
Accepted 17 June 2013

Using a standard sample to estimate the X-ray wavelength of the 1W2A SAXS beamline at BSRF

Jun Liu and Zhihong Li*

Beijing Synchrotron Radiation Facility, Institute of High Energy Physics, Chinese Academy of Sciences, PO Box 918, Beijing 100049, People's Republic of China. E-mail: box@china.com.cn

This contribution describes a method for measuring diffraction peaks of a standard sample to estimate the incident X-ray wavelength at the 1W2A SAXS beamline at BSRF. A simple simulation has been performed to establish the factors influencing the accuracy of the wavelength measurement. Appropriate measurement conditions and error control measures are presented. An actual experimental example further verifies the effectiveness of the simulation. This method is particularly suitable for synchrotron radiation beamlines using bent triangular crystal monochromators.

Keywords: SAXS; wavelength estimation; standard sample.

1. Introduction

The incident X-ray wavelength or energy is one of the characteristic parameters of any X-ray instrument. With double-crystal monochromators it can sometimes easily be calibrated using the absorption edge of a standard sample (Schilling *et al.*, 1995). However, for beamlines with a bent triangular crystal monochromator (Zheng *et al.*, 1995) or beamlines with a double-crystal monochromator where the wavelength does not correspond to an edge, one has to find other methods to estimate the wavelength. The new beamline 1W2A at Beijing Synchrotron Radiation Facility (BSRF) is a fixed-energy (about 8 keV) beamline dedicated to small-angle X-ray scattering (SAXS). This beamline shares the same synchrotron radiation source with the protein crystallography beamline 1W2B through a triangular bending Si(111) crystal monochromator. In principle, one does not have to know the wavelength very accurately in SAXS because one is usually only interested in the calibration of the q- or s-axis. An accurate knowledge of the wavelength is, however, useful for absorption and scattering angle calculation. One of the possible methods is to measure the diffraction peak(s) of a standard sample. This short contribution reports the results of a simple theoretical simulation and an experimental verification. The method may be applied to similar beamlines.

2. Theory and simulation

2.1. Wavelength and error

A schematic diagram of a typical scattering or diffraction experiment is shown in Fig. 1. The monochromatic X-rays irradiate the sample and the scattering or diffraction signals are recorded by a detector. Obviously, there exists a simple mathematical relation (1) valid if the direct beam is perpendicular to the detector plane,

$$2\theta = \arctan(P/L), \tag{1}$$

where 2θ is the scattering or diffraction angle, P is the radius of the scattering or diffraction ring on the detector plane, and L is the sample-to-detector distance.

Assuming a known crystalline sample with distinct diffraction peaks is used for the experiment, Bragg's law (Bragg & Bragg, 1913), (2), states that the incident X-ray wavelength λ can be derived from the distance d between atomic layers in the crystal and the diffraction angle 2θ,

$$n\lambda = 2d\sin\theta, \tag{2}$$

where n is an integer. Combining (1) and (2) one obtains (3),

$$n\lambda = 2d\sin\frac{\arctan(P/L)}{2}. \tag{3}$$

For a given standard sample with known d-spacing, once the P and L values for a known diffraction peak are measured, one can derive λ using (3). According to the error propagation principle (Ma & Wang, 2009), the error on λ (named $\Delta\lambda$) depends on P, L and their errors ΔP and ΔL,

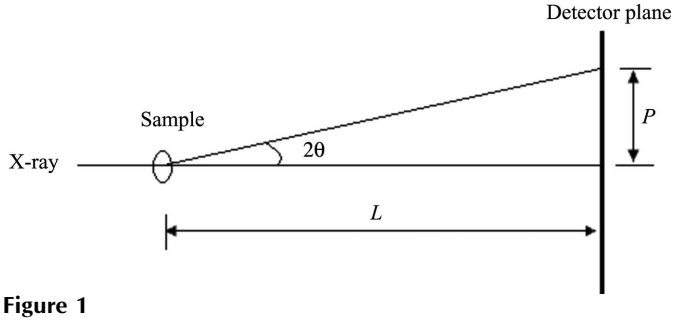

Figure 1
Schematic diagram of a typical X-ray diffraction or scattering.

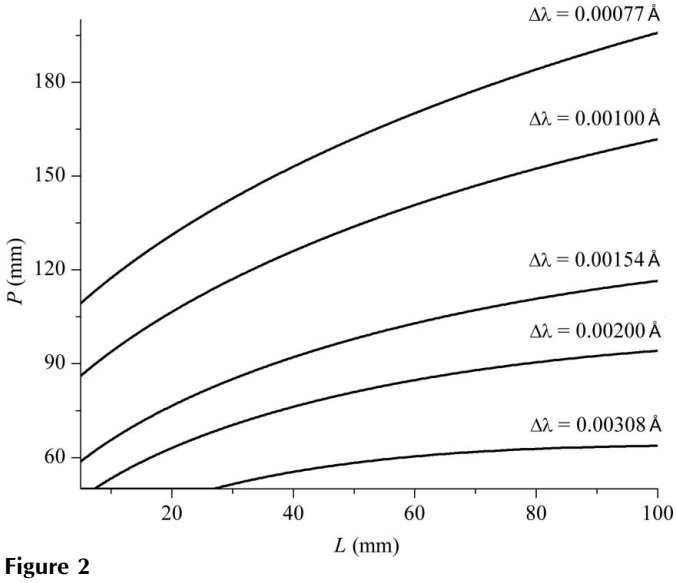

Figure 2
Variation of $\Delta\lambda$ with L and P assuming $\Delta P = \Delta L = 0.10$ mm.

$$\Delta\lambda = \frac{\partial\lambda}{\partial P}\Delta P + \frac{\partial\lambda}{\partial L}\Delta L = \left|2d\cos\left[\frac{\arctan(P/L)}{2}\right]\right| \frac{P\Delta L + L\Delta P}{2\left[1+(P/L)^2\right]L^2}. \quad (4)$$

Equation (4) shows that $\Delta\lambda$ varies linearly with both ΔP and ΔL. Fig. 2, derived from (4) assuming $\Delta P = 0.10$ mm and $\Delta L = 0.10$ mm, illustrates the variation of $\Delta\lambda$ with L and P. For a given value of L, the greater P, the smaller $\Delta\lambda$, and, for a given value of P, the shorter L, the smaller $\Delta\lambda$. So for a given expected value of $\Delta\lambda$, P and L should lie in a limited range. For example, if one expects $\Delta\lambda \leq 0.00154$ Å ($\lambda \times 1‰$), then the combination of P and L must be above the curve for $\Delta\lambda = 0.00154$ Å in Fig. 2. Supposing $L = 100$ mm, one has to keep $P \geq 116.45$ mm. Conversely, if $P = 116.45$ mm, one has to keep $L \leq 100$ mm.

P and ΔP are usually easily estimated from the known pixel size or point spread function of the detector. But L and ΔL are difficult to measure accurately, as the real position of the photosensitive plane of the detector is rarely known. In the case of a Mar165 CCD detector with a pixel size of 79 µm, ΔP may be about 0.1 mm. ΔL mainly depends on the measurement method. When measuring with a tape or ruler, ΔL is large and about several millimetres. Therefore, the key for the determination of λ with expected error $\Delta\lambda$ is measuring L with a limited error ΔL.

2.2. Sample-to-detector distance and error

The sample-to-detector distance L can be determined with a standard sample. Either of the two simple schemes shown in Fig. 3 can be used. In the first, the standard sample position is fixed and two independent diffraction peaks are measured once (see Fig. 3*a*). In the second, the standard sample position is displaced and one diffraction peak is measured twice (see Fig. 3*b*).

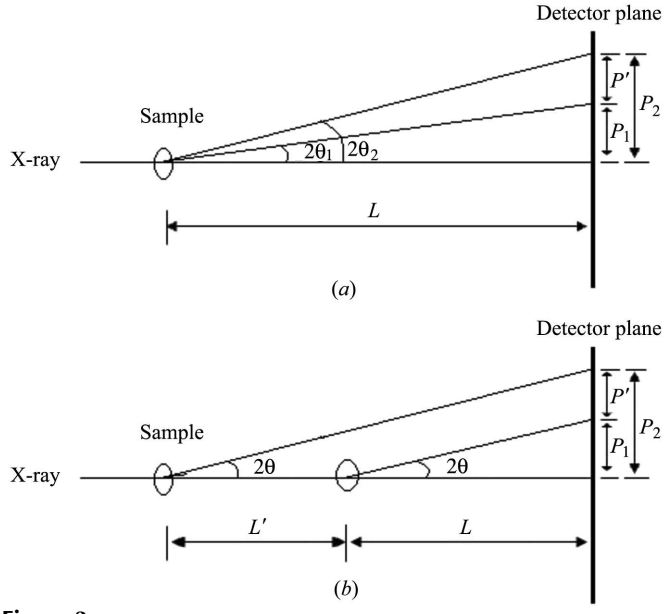

Figure 3
Schematic diagram of set-ups for determining the sample-to-detector distance. (*a*) The sample position is fixed and two independent diffraction peaks are measured once. (*b*) The sample is displaced and one diffraction peak is measured twice.

For the first scheme, the following relation can be derived from (3),

$$d_1 \sin\left[\frac{\arctan(P_1/L)}{2}\right] = d_2 \sin\left[\frac{\arctan(P_2/L)}{2}\right]. \quad (5)$$

After measuring P_1 and P_2 for two different diffraction peaks with known d_1 spacing and d_2 spacing, L can be derived from (5). Equation (5) is a transcendental equation, which has no analytical solution, but a numerical solution. According to the error propagation principle, ΔL depends on P_1, P_2, ΔP_1 (error of P_1), ΔP_2 (error of P_2) and L,

$$\Delta L = \left\{\left|d_1\cos\left[\frac{\arctan(P_1/L)}{2}\right]\frac{L}{L^2+P_1^2}\right|\Delta P_1 + \left|d_2\cos\left[\frac{\arctan(P_2/L)}{2}\right]\frac{L}{L^2+P_2^2}\right|\Delta P_2\right\} \Bigg/ \left\{\left|d_1\cos\left[\frac{\arctan(P_1/L)}{2}\right]\frac{P_1}{L^2+P_1^2} - d_2\cos\left[\frac{\arctan(P_2/L)}{2}\right]\frac{P_2}{L^2+P_2^2}\right|\right\}. \quad (6)$$

Further setting $P_2 = P_1 + P'$ and $\Delta P_1 = \Delta P_2 = 0.10$ mm, one can derive the variation of ΔL with L and P' as shown in Fig. 4. For a given value of L, the greater P', the smaller ΔL; for a given value of P', the shorter L, the smaller ΔL. Therefore for an expected value ΔL, P' and L should lie in a limited range. For example, if one expects $\Delta L \leq 0.10$ mm to match $\Delta\lambda \leq 0.00154$ Å, then the combination of P' and L must be above the curve for $\Delta L = 0.10$ mm in Fig. 4. Supposing $L = 44.00$ mm,

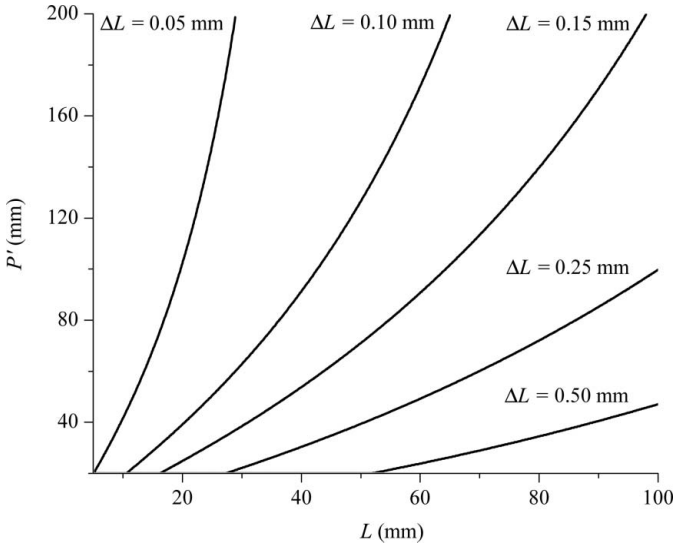

Figure 4
Variation of ΔL with L and P' assuming $P_2 = P_1 + P'$ and $\Delta P_1 = \Delta P_2 = 0.10$ mm.

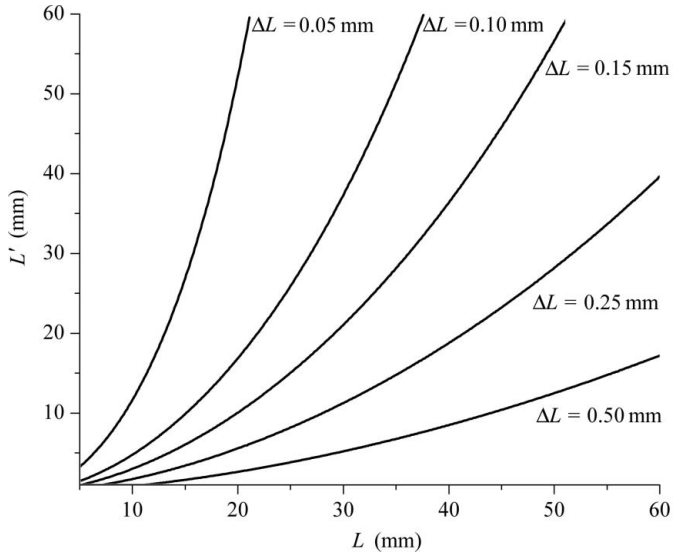

Figure 5
Variation of ΔL with L and L' assuming $\Delta P_1 = \Delta P_2 = 0.10$ mm and $\Delta L' = 0.01$ mm.

one has to keep $P_1 \geq 94.49$ mm according to (4) and Fig. 2, $P' \geq 104.40$ mm and $P_2 \geq 198.89$ mm according to (6) and Fig. 4. This means that the detector must have an active area with diameter or length larger than 198.89 mm. On the contrary, if $P_1 = 94.49$ mm, $P' = 104.40$ mm and $P_2 = 198.89$ mm, one has to keep $L \leq 44.00$ mm. It can be concluded that, to match the specific restriction of $\Delta\lambda$ (*e.g.* 1‰), L is limited (for instance $L \leq 44.00$ mm) by the particular detector (say 200.00 mm diameter of active area) based on the scheme of Fig. 3(*a*).

For the second scheme, it is easy to obtain the relationship in (7) from Fig. 2(*b*),

$$\frac{P_1}{L} = \frac{P_2}{L + L'}. \tag{7}$$

After measuring P_1, P_2 and L' with the corresponding errors ΔP_1, ΔP_2 and $\Delta L'$, respectively, L can be derived from (7). ΔL depends on P_1, P_2, L', ΔP_1, ΔP_2 and $\Delta L'$,

$$\Delta L = \frac{P_2 L'}{(P_2 - P_1)^2}\Delta P_1 + \frac{P_1 L'}{(P_2 - P_1)^2}\Delta P_2 + \frac{P_1}{P_2 - P_1}\Delta L'. \tag{8}$$

Further setting $\Delta P_1 = \Delta P_2 = 0.10$ mm and $\Delta L' = 0.01$ mm [this is easily achieved using a precise (several micrometers) displacement stage], one can derive the variation of ΔL with L and L' as shown in Fig. 5. For a given value of L, the larger L', the smaller ΔL; for a given value of L', the shorter L, the smaller ΔL. Therefore for a given expected value of ΔL, L' and L should lie in a certain limited range. For example, if one expects $\Delta L \leq 0.10$ mm to match $\Delta\lambda \leq 0.00154$ Å, then the combination of L' and L must be above the curve of $\Delta L = 0.10$ mm in Fig. 5. Supposing $L = 31.00$ mm, then one has to keep $P_1 \geq 85.78$ mm according to equation (4) and Fig. 2, and $L' = 39.95$ mm and $P_2 \geq 196.33$ mm according to equation (8) and Fig. 5. This means that the detector must have an active area with diameter or length larger than 197.00 mm. Conversely, if $P_1 = 85.78$ mm, $L' = 39.95$ mm and $P_2 = 196.33$ mm, then one has to keep $L \leq 31.00$ mm. It can be concluded that, to match the specific restriction of $\Delta\lambda$ (*e.g.* 1‰), L is still limited (for instance $L \leq 31.00$ mm) by the particular detector (say 197.00 mm diameter of active area) based on the scheme of Fig. 3(*b*).

The choice between the above schemes to determine the sample-to-detector distance with limited errors depends on the actual situation. In the first scheme the position of the standard sample is fixed while in the second scheme the standard sample must be accurately displaced. The first scheme measures two diffraction peaks with different *d*-spacings once, while the second measures the same diffraction peak of the standard sample twice. Both schemes avoid the direct influence of the error of the sample-to-detector distance on the error on the wavelength calculation.

The use of several more diffraction peaks of the standard sample to determine the sample-to-detector distance is not discussed here, but it could be analyzed with methods similar to those above.

2.3. Influence of the tilt of the detector

The schemes presented above are based on the situation where the detector is perpendicular to the beam (see Fig. 1). If the angle between the detector and the direct beam is α, it is easy to derive the following relationship,

$$P = \frac{\sin(2\theta)}{\sin(2\theta + \alpha)}\, L. \tag{9}$$

Then the error of P can be computed according to the error propagation principle,

$$\Delta P = \left|\frac{-\sin(2\theta)\cos(2\theta + \alpha)}{\sin^2(2\theta + \alpha)}\right| L\, \Delta\alpha, \tag{10}$$

where $\Delta\alpha$ is the error on α and just the tilt angle of the detector. Apparently, there exists a linear relation between ΔP and $\Delta\alpha$. One can further derive the ratio of $\Delta P/P$,

$$\frac{\Delta P}{P} = \left|-\cot(2\theta+\alpha)\right| \Delta\alpha. \qquad (11)$$

Equation (11) indicates that $\Delta P/P$ depends on $\Delta\alpha$ by a linear relation. Assuming $\alpha = 90^\circ$, then one can derive the variation of $\Delta P/P$ with 2θ and $\Delta\alpha$ as shown in Fig. 6. It can be seen that the larger $\Delta\alpha$, then the larger $\Delta P/P$. Obviously, $\Delta\alpha$ has a distinct influence on the error on P especially for large diffraction angles. The maximum allowable value for $\Delta\alpha$ depends on the expected values of ΔP. For example, if $2\theta = 70^\circ$ and $P = 100$ mm, then one has to set $\alpha \leq 0.02^\circ$ to keep $\Delta P \leq 0.10$ mm. One should thus pay great attention to control the tilt angle of the detector for wide angle diffraction measurement. Modern mechanical displacements and consoles enable the detector attitude to be adjusted accurately. The perpendicularity of the detector to the beam is easy to verify by the symmetry of a diffraction ring of a given sample, so $\Delta\alpha$ can easily reach the acquirement of ΔP.

Table 1
Experimental conditions and results with the scheme in Fig. 3(*a*).

d (Å)	P (mm)	ΔP (mm)	L (mm)	ΔL (mm)	λ (Å)	Δλ (Å)
1.221	70.729	0.100	15.064	0.077	1.536414	0.001267
1.169	109.480	0.100	15.064	0.077	1.536413	0.000720

Table 2
Experimental conditions and results with the scheme in Fig. 3(*b*).

d (Å)	L' (mm)	$\Delta L'$ (mm)	P (mm)	ΔP (μm)	L (mm)	ΔL (mm)	λ (Å)	Δλ (Å)
1.169	6.000	0.010	64.485	0.100	8.836	0.0688	1.536908	0.001106
1.169	6.000	0.010	108.273	0.100	14.836	0.0695	1.536908	0.000664

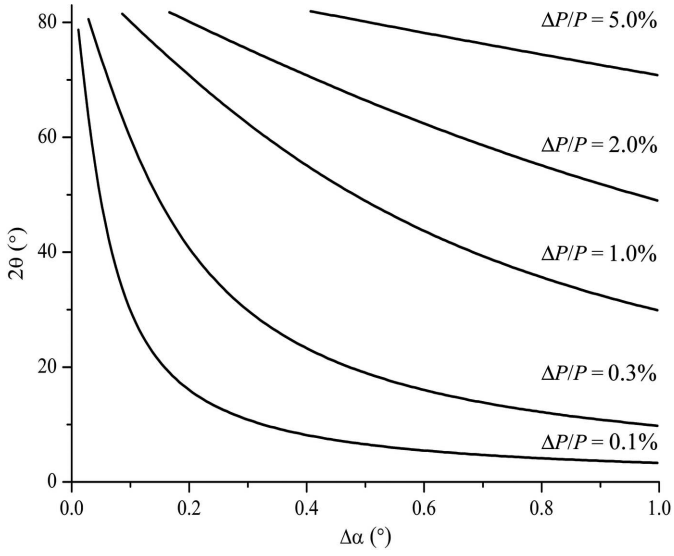

Figure 6
Variation of $\Delta P/P$ (% error on P) with diffraction angle 2θ and the error on α.

3. Experimental example

The experiment has been performed at the 1W2A SAXS station at BSRF. Aluminium powder (purity 99%) (Tianjin Heowns Biochem LLC) was used as a standard sample with distinct diffraction peaks (the standard data are from JCPDS 65-2869) and mounted on a high-precision (∼5 μm) positioning stage. An area detector (Mar 165 CCD), set perpendicular to the incident X-rays, was used to record the diffraction pattern. The experimental conditions were based on the previous considerations. The partial diffraction profiles of the aluminium powder sample with the schemes of Figs. 3(*a*) and 3(*b*) are shown in Figs. 7(*a*) and 7(*b*), respectively. The detailed experimental conditions and results are listed in Tables 1 and 2.

The results shows that the calculated X-ray wavelength values from both schemes in Fig. 3 are very close to each other and to the design value of 1.54 Å for the Si(111) crystal

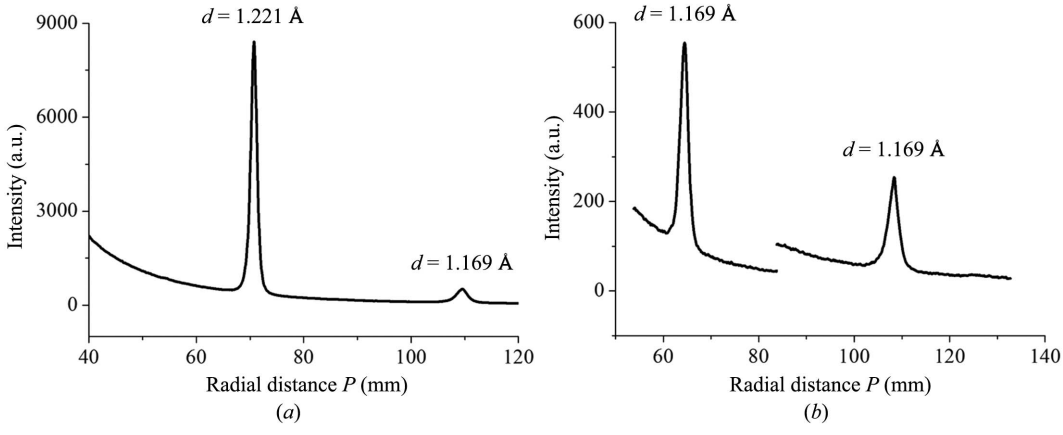

Figure 7
(*a*) Partial diffraction pattern of aluminium powder performed with the scheme in Fig. 3(*a*) at the 1W2A SAXS station at BSRF. (*b*) Partial diffraction pattern of aluminium powder performed with the scheme in Fig. 3(*b*) at the 1W2A SAXS station at BSRF.

monochromator. The small difference might result from a small alignment error. All $\Delta\lambda/\lambda$ values are lower than 1‰.

4. Conclusion

This presentation describes how to estimate the X-ray wavelength from a monochromatic X-ray beam or instrument especially in the case where this cannot be easily done using the absorption spectrum of a metallic foil (*e.g.* when using a bent triangular crystal monochromator). Two possible protocols are described in which either one or two independent diffraction peaks of a standard sample are measured. Analysis of the resulting wavelength value error is performed in terms of error propagation of several measurement quantities. Neither protocol needs a direct measurement of the distance between the sample and the detection plane which is rarely known with precision. The limitation to the measurement quantities depends on the expected error on the wavelength. Although based on simple well known geometrical equations, the presentation provides new insights into the interplay between the various parameters, and the results could be useful for optimizing the scheme and operation of such beams.

We are grateful to Dr Michel Koch (EMBL, Hamburg, Germany) for valuable advice. We acknowledge the financial support of this study by the Foundation of National Nature Science (Grant Nos. 11079041, 10835008, 21176255, 10979005, 10979076 and 111107903928).

References

Bragg, W. H. & Bragg, W. L. (1913). *Proc. R. Soc. A*, **88**, 428–438.
Ma, H. & Wang, J. (2009). *Instrument Accuracy Theory*. Beihang University Press.
Schilling, P. J., Morikawa, E., Tolentino, H., Tamura, E., Kurtz, R. L. & Cusatis, C. (1995). *Rev. Sci. Instrum.* **66**, 2214–2216.
Zheng, W., Jiang, X., Wu, J., Jing, Y. & Liu, G. (1995). *High Energy Phys. Nucl. Phys.* **19**, 858–864.